designs

MDPI

Review

A Review of the Current State of the Art of Polyether Ether Ketone (PEEK) Composite Based 3D-Printed Biomedical Scaffolds

Rajesh Surendran [1], Sithara Sreenilayam Pavithran [2,3,*], Anugop Balachandran [4], Sony Vijayan [3], Kailasnath Madanan [4] and Dermot Brabazon [2,3]

[1] Department of Physics, Mar Ivanios College (Autonomous), Thiruvananthapuram 695015, India; rajesh.s@mic.ac.in
[2] I-Form, Advanced Manufacturing Research Centre, Dublin City University, Glasnevin, D09 Dublin, Ireland; dermot.brabazon@dcu.ie
[3] Advanced Processing Technology Research Centre, School of Mechanical and Manufacturing Engineering, Dublin City University, Glasnevin, D09 Dublin, Ireland; sony.vijayan@dcu.ie
[4] International School of Photonics, Cochin University of Science and Technology, Kochi 682022, India; anugopb@cusat.ac.in (A.B.); kailas@cusat.ac.in (K.M.)
* Correspondence: sithara.sreenilayam@dcu.ie

Abstract: Three-dimensional printing or additive manufacturing (AM) has enabled innovative advancements in tissue engineering through scaffold development. The use of scaffolds, developed by using AM technology for tissue repair (like cartilage and bone), could enable the growth of several cell types on the same implant. Scaffolds are 3D-printed using polymer-based composites. polyether ether ketone (PEEK)-based composites are ideal for scaffold 3D printing due to their excellent biocompatibility and mechanical properties resembling human bone. It is therefore considered to be the next-generation bioactive material for tissue engineering. Despite several reviews on the application of PEEK in biomedical fields, a detailed review of the recent progress made in the development of PEEK composites and the 3D printing of scaffolds has not been published. Therefore, this review focuses on the current status of technological developments in the 3D printing of bone scaffolds using PEEK-based composites. Furthermore, this review summarizes the challenges associated with the 3D printing of high-performance scaffolds based on PEEK composites.

Keywords: 3D printing; biomaterial; implants; PEEK composites; additive manufacturing

Citation: Surendran, R.; Pavithran, S.S.; Balachandran, A.; Vijayan, S.; Madanan, K.; Brabazon, D. A Review of the Current State of the Art of Polyether Ether Ketone (PEEK) Composite Based 3D-Printed Biomedical Scaffolds. *Designs* **2023**, *7*, 128. https://doi.org/10.3390/designs7060128

Academic Editor: Mahdi Bodaghi

Received: 26 August 2023
Revised: 23 October 2023
Accepted: 31 October 2023
Published: 10 November 2023

1. Introduction

Additive manufacturing (AM) technologies have advanced greatly over the past few decades. In these technologies, products or three-dimensional (3D) parts are developed from their computer-aided-design (CAD) models [1–3]. The parts to be printed are built up in a layer-by-layer scheme on a plane designated as the X–Y plane, and the layers are added in the orthogonal Z-direction. 3D printing opens up new possibilities for fabricating complex structures using multiple materials [4,5] and reduces the design–manufacturing cycle, which in turn reduces the production costs and the material wastage. According to the nature of materials and parts development, there are seven different classes of AM techniques (Figure 1). Many parameters affect the quality of the final parts in the AM processes. To manufacture high-quality AM products, a good understanding of the process and material properties is essential. In recent years, the quality control/checking of AM structures has received much attention from manufacturing industries to make sure that the parts developed have the required specific functional properties [6–8]. For example, unwanted porosity in AM parts adversely affects their mechanical performance [9,10]. Recent studies have demonstrated the production of high-density parts (>99.8%) with the utilization of improved control systems [11]. The development of new AM materials for manufacturing critical AM structural parts is becoming increasingly important. AM technologies are used in the aerospace [12],

automotive [13], medical science [14], and printed electronics [15,16] industries. The application of AM technologies in the biomedical field includes the production of customized prostheses, surgical and assistive tools, implants, instruments, pre-operative surgical planning and disease diagnosis and treatments [17]. Using 3D printing methods, functional tissue can be assembled from cells and scaffold materials. In tissue engineering, a 3D-printed construct would be ideal since it would be able to direct cells to migrate and proliferate, resulting in functional tissue.

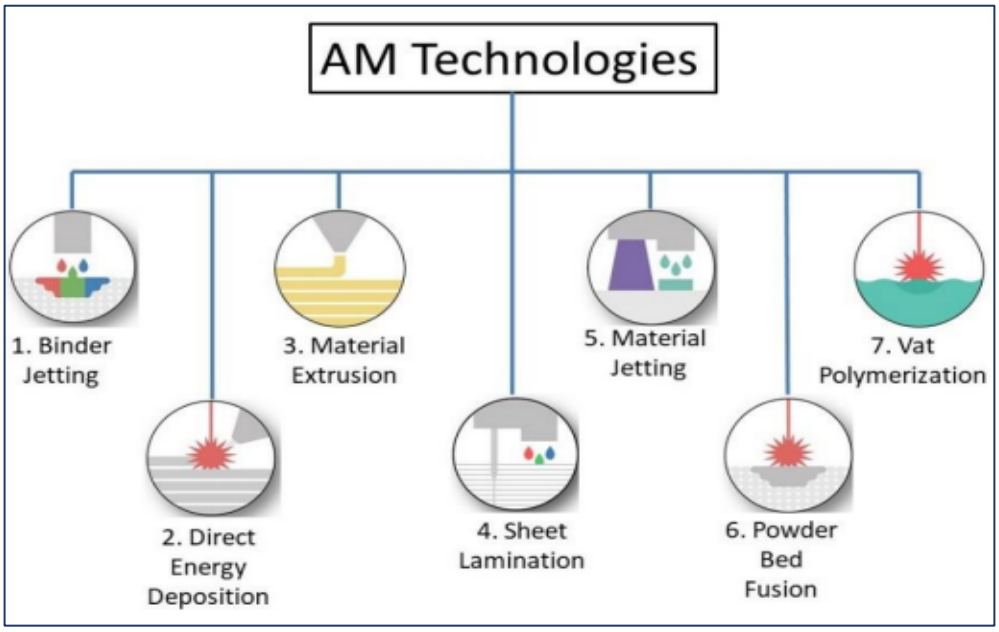

Figure 1. Additive manufacturing (AM) classification [18].

A combination of material engineering and tissue engineering can be used to treat human body parts losses [19]. In tissue engineering technology, scaffolds, or 3D porous biomaterials, play an important role [20]. In scaffold fabrication, biomaterials made from synthetic polymers, natural polymers, ceramics, composites, and metals are engineered in such a way as to facilitate the cellular interactions required for the generation of new functional tissues [21–23]. Polycarbonate, poly(D,L-lactic-co-glycolic acid), and poly(e-caprolactone) are examples of synthetic polymer-based biomaterials that can be applied to scaffold development. There are several natural polymers that can be used for this application, including silk, keratin, chitosan, and alginate. In terms of ceramics, calcium sulphate and calcium silicate are suitable for scaffold fabrication. Titanium (Ti–6Al–4V) and cobalt–chromium (Co–Cr) are two examples of metal materials used for the above-mentioned application. Each scaffold material has its own specific properties (e.g., mechanical, chemical, or physical), and it is selected according to the properties required for the specific biomedical implant and fabrication process [24–26]. To maintain mechanical characteristics similar to those of nearby tissue, it is necessary for the scaffold to temporarily resist external loads or stresses during the regeneration process of new tissue.

Tissue engineering scaffolds can be manufactured using a variety of techniques. Traditional manufacturing processes, such as phase separation [27], freeze-drying [28,29], salt leaching [30,31], or gas forming [32,33], do not offer an optimal solution to maintain its porous structure effectively. Pore size and porosity in scaffolds affect the delivery of oxygen and nutrients and enhance the growth of cells [34]. Through its porous structure, the implant gains mechanical stability by enabling mechanical interlocking between scaffolds and neighboring tissues [35]. Additionally, the pores' network structure aids in new tissue growth. Despite being good for nutrient exchange, high porosity negatively affects a scaffold's mechanical properties [36]. The mechanical and nutrient mass transport functions of a scaffold system must be balanced to achieve optimal performance. The

final porosity and size of pores should therefore be considered at the design stage of a scaffold based on its intended application. Recently, there has been much interest in bone scaffold generation with customized architecture, strength, macro/micro-structure, wettability, cellular responses, etc. The AM process can be used to produce patient-specific scaffolds [37]. Recent studies by Ali Bahri et al. have reported porous scaffold 3D printing with controlled pore sizes and well-defined external and internal structures [38,39]. Metals like cobalt–chromium, titanium, and stainless steel alloys are typically used in orthopaedic scaffold 3D printing for bone repair or replacement since they are relatively strong and biocompatible [40,41]. The selection of a metal for use as an implant scaffold material is restricted due to its biodegradation inside the body, as well as the lack of the 3D printing production technique having been developed for printing particular metals [42,43]. Even though scaffolds are mechanically strong with small amounts of metal, biodegradability and compatibility are important issues to consider [44–46]. This problem can be solved by developing biodegradable metal materials. Metal matrix composites based on zinc, iron, magnesium, and calcium are an example of such materials. [47,48]. For scaffold development, iron- and magnesium (Fe-Mn)-based metal matrix composites have already been used. Fe-Mn scaffolds developed by inkjet 3D printing show high tensile properties like bone, and are biodegradable. Such new scaffolds should allow related implant site-specific biological cells to proliferate and differentiate. Due to their good biocompatibility and mechanical properties, ceramic materials containing both non-metallic and metallic components are used for scaffold 3D printing [49]. The ability to generate apatite mineralization makes ceramics attractive for scaffold development [50]. The ceramic material form that is normally found in human bone and teeth is hydroxyapatite (HA) [51]. In scaffold 3D printing and regenerative medicine, this material or other materials with similar properties have received much attention due to their mechanical properties. The positive biocompatibility and cell growth assistance properties of HA have been demonstrated in many studies [52,53]. The ceramics used in 3D printing scaffolds include calcium phosphate, calcium sulphate, calcium silicate, and tricalcium phosphate (Figure 2a) [54–56]. By using calcium phosphate ceramic in combination with HA and tricalcium phosphate, studies have reported scaffold manufacturing with a geometric accuracy of better than 97.5% when compared to computer-aided design (CAD) files. To fabricate models using 3D printing techniques, CAD designs are required. As this offers a high-resolution design and pore sizes as low as 300 µm, such ceramics are considered as suitable materials for scaffold fabrication and cell growth. However, for the load-bearing capabilities of ceramics in the 3D printing of scaffolds, further research and development studies are required.

Polymer-based composites are of key importance for scaffold 3D printing. Both thermosets and thermoplastics have been used extensively for this application [37,57]. Examples of such polymers are gelatin methacrylate (GelMA), poly(ethylene glycol) diacrylate (PEGDA), poly(D,L-lactic-co-glycolic acid) (PLGA), polyglycolic acid (PGA), poly(hydroxy butyrate), polycaprolactone (PCL) and poly(propylene fumarate) [58,59]. Among these, the synthetic polymers PLGA and PCL show low toxicity during material degradation [60]. To avoid materials that cause inflammation in tissue regeneration, it is essential to understand the inflammatory response [61,62], as a number of these polymers exhibit fast biodegradation [63]. PCL- and PLGA-based scaffolds have been 3D-printed with pore sizes of ∼300 µm (Figure 2b,c) [64].

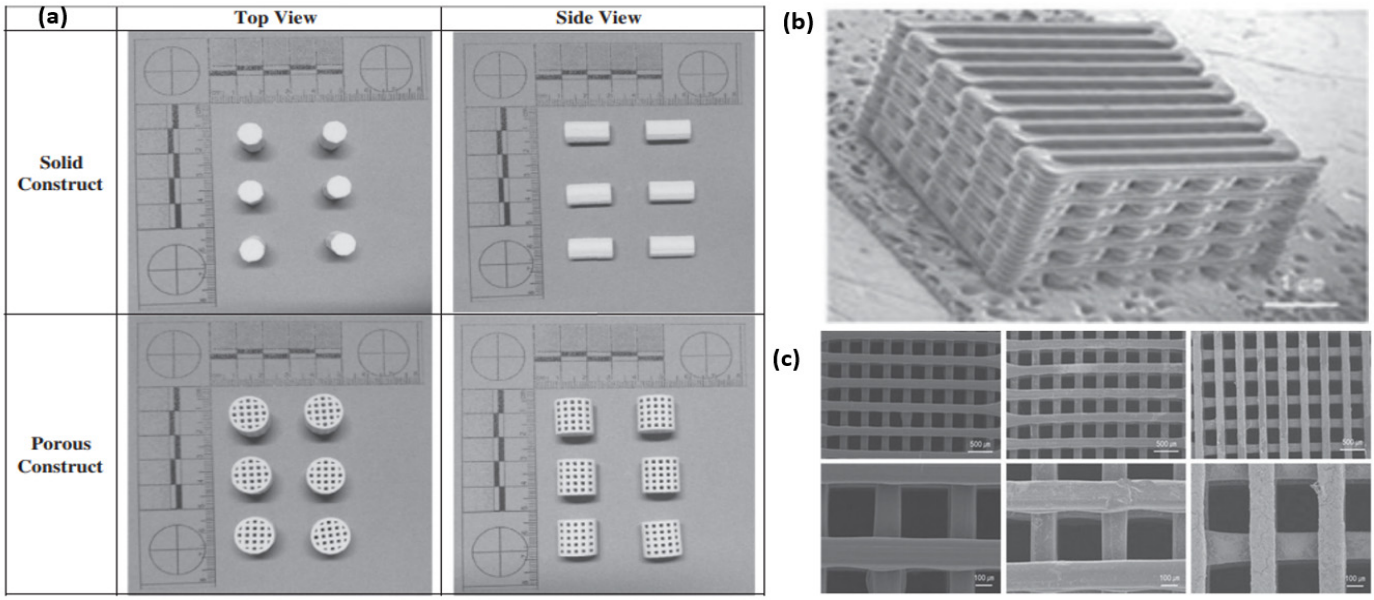

Figure 2. (**a**) Calcium sulphate and HA-based porous structures developed using thermal inkjet 3D printer [55]. Copyright © 2014 with permission from Elsevier. PCL/PLGA scaffold developed using fused deposition modeling (FDM) printer showing (**b**) macroscopic and (**c**) higher magnification SEM images [64]. Copyright © 2012 with permission from Elsevier.

Collagen, a type of natural polymer, is the most common candidate used for tissue engineering, along with corn starch, dextran, proteins, and polysaccharides [65]. Collagen (an insoluble fibrin found in human body tissues)-based 3D-printed scaffolds have been reported in many studies [66,67]. Various methods can be used to develop collagen scaffolds [68]. In 2022, Zhengwei Li et al. reported a technique to produce an in situ mineralized scaffold based on collagen for guided bone regeneration [39]. The mineralization process in this work involved electrospinning mineral ions in a collagen solution. In one of the works, Xiao-Hong Li et al. reported a collagen–silk fibroin-based scaffold implant for nerve-repairing applications [69]. In their study, they focused on two techniques, such as freeze-drying technology and 3D printing, and it was found that rats' neurological function, based on locomotor performance and electrophysiological analysis, was significantly enhanced by the implant made via the 3D printing method compared to the other implant. One study by Xiaoyi Lan et al. showed a bioprinting technique to develop collagen-based tissue-engineered nasal cartilage (Figure 3b) [70]. For this work, they used human nasoseptal chondrocytes and bovine type I collagen hydrogel for FRESH-inspired bioprinting, and suggested that this is a promising strategy for exploring further for providing autologous nasal cartilages for nasal cartilage reconstructive surgeries. The use of composite materials provides higher mechanical properties to the 3D-printed scaffold. The 3D printing of scaffolds made of bioactive calcium phosphate glass and polylactic acid (PLA) composite was reported in one study. In this case, an extrusion-based 3D printer was used to develop scaffolds with high porosity [71]. The utilization of composites is important in the development of the 3D-printed extracellular matrix of scaffolds. Figure 3a is a schematic of the scaffold 3D printing process [72] and Figure 3b is the bioprinting process based on collagen ink [70]. Table 1 presents some examples of biomedical scaffold materials, methods, and applications.

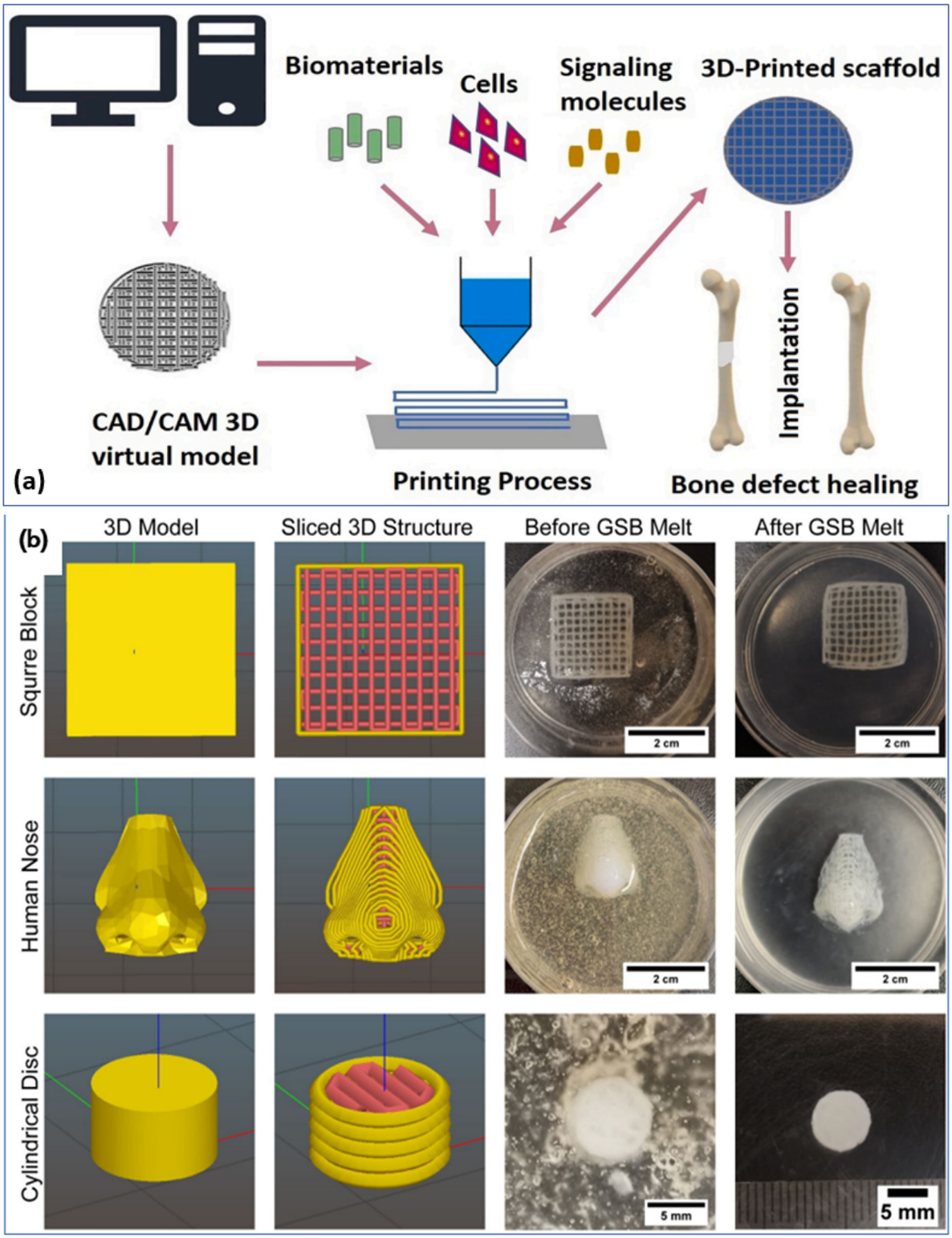

Figure 3. (**a**) Schematic of the scaffold 3D printing process [72]. Copyright © 2021 with permission from Elsevier. (**b**) Bioinspired tissues made up of collagen bio-ink in a gelatin bath using a FRESH bioprinting technique [70]. Copyright © 2021 the authors.

Table 1. Selected examples of materials, methods, and applications of biomedical scaffolds.

	Material	Application	Fabrication Methods	Ref.
Metal/metal alloys	Ti-6Al-4V	Bone implant	electron beam melting and selective laser melting	[73]
	Ti-6Al-4V	Dental implants	Laser Beam Melting	[74]
	Ti-6Al-4V	Segmental bone reconstruction	Electron beam melting	[75]
	Stainless steel	Bone implant	Selective Laser Melting	[76]
Ceramics	Tricalcium phosphate	Bone implant fabrication	Inkjet printing	[77]
	α-tricalcium phosphate	Maxillofacial bone defect reconstruction	3D printing	[78]
	Calcium carbonate	Adhesion, growth, and proliferation of osteoblast MC_3T_3 cells	Supercritical CO_2-based process	[79]
	β-tricalcium phosphate	Hard tissue repair	3D gel-printing	[80]
	Hydroxy apatite	Bone repair	DLP	[81]
	Calcium phosphate	Skull bone tissue reconstruction	Inkjet printing	[82]
	CaO-SiO_2-P_2O_5-B_2O_3 glass-ceramic	Maxillofacial bone defect reconstruction	3D printing	[83]
	Alumina	bone implant	Lithography-based Ceramics Manufacturing (LCM) technology	[84]
Composites	b-tricalcium phosphate and poly (D,L)-lactide	Fabrication of biodegradable bone implants	Selective Laser Melting	[85]
	Ti-6Al-4V, magnesium-calcium silicate (Mg-CS), and chitosan (CH)	Orthopedic	Laser melting deposition	[86]
	Polylactic acid/ biphasic calcium phosphate	Bone substitutes	Fused Deposition Modeling	[87]
	mPCL and TCP	Long bone reconstruction	3D printing	[88]
	Barium titanate and hydroxyapatite	Bone implant	3D printing	[89]
	Poly-lactic acid and nano-hydroxyapatite	bone scaffold	Fused Deposition Modelling	[90]
	30%HA-70% b-TCP BCP	Dental bone defect augmentation	3D printing	[91]
Polymers	Collagen and fibrinogen	Cartilage	Inkjet printing	[92]
	Methacrylated hyaluronan and methacrylated gelatin	Cardiac	Extrusion	[93]
	Gelatin and fibrinogen	Vascular	Extrusion	[94]
	Cell-laden collagen core and alginate sheet	Liver	Extrusion	[95]
	Gelatin, alginate, EGF, and dermal homogenates	Sweat gland	Extrusion	[96]

Many companies have started using the polyether ether ketone (PEEK) material for 3D printing as it exhibits unique qualities. Where traditional production methods or metallic materials are difficult to use, PEEK is a good choice for the low-volume production of required designs. Due to its low moisture absorption, easy sterilization, and biocompatibility,

the use of PEEK materials in medical devices has increased in recent years. 3D-printed PEEK based implants and scaffolds have been developed and used without any complications. Recent review articles on PEEK discuss its use in soft and hard tissue engineering [97], as well as orthopedics [98]. As a detailed review of the recent developments in PEEK composites and the 3D printing of scaffolds has not been published, this review provides an overview of the recent advances in PEEK and PEEK composite materials for bone scaffold production as well as the 3D printing techniques used for processing these materials.

2. Poly Ether Ether Ketone (PEEK) for Scaffolds

Polyether ether ketone or PEEK is a biocompatible polymer extensively used for various applications, especially in the biomedical field. PEEK, chemically recognized as a linear poly (arylether ketone), is a high-performance, melt-processable aromatic polymer [99,100]. PEEK molecules are oriented in a planar zig-zag conformation with an orthorhombic crystal structure [101]. Because of its semicrystalline nature, PEEK finds a wide range of biomedical supporting applications such as lumbar cervical, thoracic, spinal, trauma and orthopedic implants. PEEK is chemically inert, and it is insoluble at room temperature (water solubility: 0.5 w/w %.) in all conventional solvents except for 98% sulfuric acid. It is very important to consider the chemical reaction between bone tissue and implant, as this leads to degradation and cytotoxicity (meaning how toxic the implant is to cells). Cells are damaged or even killed by cytotoxic materials. With the addition of various fillers, the modulus of elasticity or Young's modulus of PEEK, i.e., 3–4 GPa, can be increased to be like that of human cortical bone (7–30 GPa). The porosity of cortical bone, or dense or compact bone, is only 5–15% [102]. The fundamental elastic modulus property measures a material's resistance to elastic deformation under load or stress, and that determines a material's capability to hold its shape [102]. As the mechanical environment influences bone growth, the scaffold's Young's modulus, or modulus of elasticity, plays a critical role in enhancing bone formation. A mismatching of the Young's modulus values between the adjacent bone and the implant can lead to fracturing, osteopenia, or stress shielding [103,104]. PEEK is widely used in high-temperature engineering applications, because of its comparatively high glass transition temperature (~145 °C) and higher melting point (~334 °C) [105]. This material shows excellent temperature stability, which could be due to its relatively stiff backbone [106]. A biomaterial's thermal stability determines how long it will last inside a body. This property is therefore an important consideration when it comes to tissue engineering. Because of its high melting and glass transition temperatures [105], this material is stable in the human body. Magnetic resonance imaging (MRI) compatibility, high resistance to gamma and electron beam radiation, and natural radiolucency are all features of this PEEK material and its composites. PEEK's properties, including high mechanical strength, thermal and radiation stability, radiolucency, chemical and wear resistance, and biocompatibility, make it a viable candidate for bone restoration and tissue engineering applications. Biocompatibility and its suitability for the biomedical field were reported in the early 1990's [107–109]. More recently, the use of PEEK for the replacement of metal implants has been demonstrated [110,111]. The early PEEK applications were for intervertebral cages. The PEEK-based cages overcame the problems that arose due to the traditional metal intervertebral cages, which were stress-shielding due to the differential elastic modulus between the metal cage and human bone. This implementation provided the foundation for PEEK's current usage in spinal implants [112,113]. Composites based on PEEK and HA have been studied by several researchers [114–121]. The formation of apatite in simulated body fluid has a direct relationship with its volume content. The mechanical properties, cell attachment, proliferation and spreading, and activity of alkaline phosphatase have been improved due to the amount of filler content in the PEEK matrix [121].

Milling, injection molding, compression molding, forming and sintering are the conventional techniques used to fabricate PEEK composites-based parts; however, precision, the complexity and control of internal geometry, and high processing costs are the limitations of these conventional processing techniques [122–131]. To overcome the above

limitations, 3D printing has been used as a forming process for fabricating PEEK-based components to produce complex shapes, which are beyond the scope of conventional technologies. The AM technique is specifically suited for the manufacturing of biomedical implants based on PEEK and its composites as patient-specific scaffolds that overcome the constraints of traditional manufacturing approaches. Selective Laser Sintering (SLS) and Fused Deposition Modeling (FDM) are widely used 3D printing methods to process PEEK and its composites [132–135]. The FDM technique, based on filament extrusion, usually uses low-melting-temperature polymers such as acrylonitrile butadiene styrene, thermoplastic polyurethane (TPU) and polylactic acid (PLA). In the work of Berretta et al., the high-temperature printing of a PEEK composite filament made up of 5% and 1% carbon nanotubes (CNTs) with a MendleMax v2.0 FDM system was examined (Figure 4a–d) [132]. According to their findings, the quality of the FDM parts depends on CNT mixing within the PEEK, printing conditions, and filaments used. In another work, the authors laser-sintered the PEEK cranial implant and analyzed its weight, dimensional accuracy, and mechanical properties (Figure 4e) [136]. They investigated the effects of the build direction (e.g., oblique, horizontal, inverted horizontal or vertical orientations) on the properties of the PEEK cranial implant. The studies show that a cranial implant developed in the horizontal direction exhibits higher geometric accuracy and compressive strength than those produced in the vertical direction.

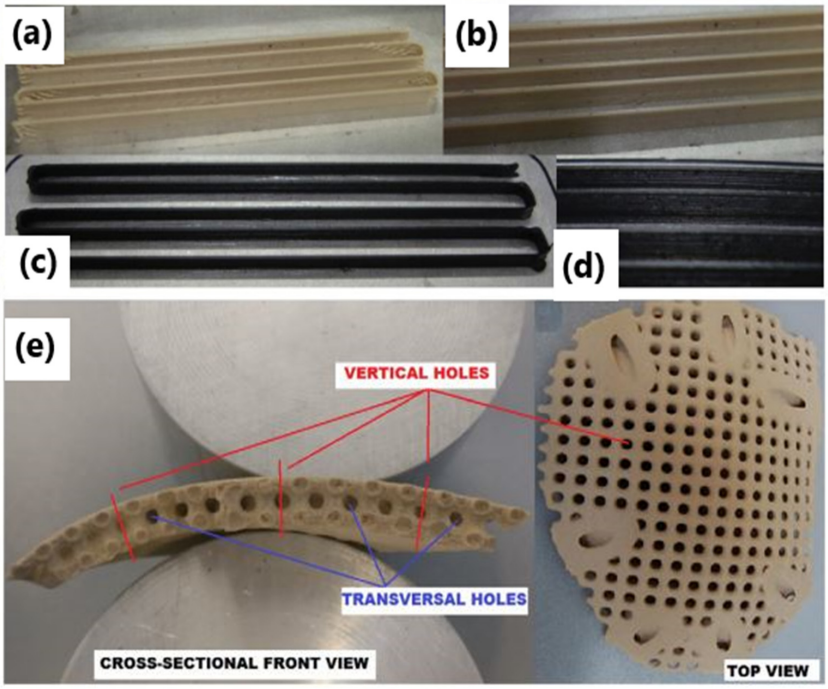

Figure 4. FDM single layer part based on (**a**,**b**) neat and (**c**,**d**) 1% CNT PEEK [57]. (**b**,**d**) Higher magnification pictures of (**a**,**c**). Copyright © 2017 with permission from Elsevier. (**e**) A 3D-printed cranial implant using the HT-LS system EOSINT P 800 [136]. Copyright © 2017 with permission from Elsevier.

Using PEEK, carbon fiber (CF)/PEEK, and glass fiber (GF)/PEEK composites, Wang et al. studied the FDM printing parameters' effects on the mechanical characteristics of the PEEK-composited FDM-produced parts [133]. This work focused mainly on the effects of nozzle temperature, platform temperature, layer thickness and printing speed on the mechanical performance of the 3D-printed parts, such as impact strength, flexural strength and tensile strength. As compared to CF/PEEK and GF/PEEK-based 3D-printed parts, pure PEEK parts showed lower tensile and flexural strengths. According to their study, the thickness of layers and printing speed affect the printed layers' strength. They noted that printing stability could be improved by lowering the print speed. Strontium- (Sr) or calcium (Ca)-doped HA, and

CNT/graphene-doped HA, are the major filler materials used to make PEEK composites for bone scaffolds. The addition of biomaterials and the incorporation of porosity into PEEK is very effective in improving osseointegration and bone implant interfaces [137–142].

In 2020, Oladapo et al. developed a cHAp/PEEK composite for the FDM-printing of scaffolds (Figure 5a) and studied the effects of cHAp on the PEEK surface [137]. The bioactivity of the developed implants was investigated by immersing them in a simulated body fluid for several days (Figure 5b–g) [137]. They found reduced biocompatibility and osseointegration around PEEK when compared to the PEEK/cHAp composite. The mechanical properties showed an improvement, with 15 wt. % cHAp as the optimum filler loading. The composite shows a better spread, adhesion, proliferation, and greater alkaline phosphatase activity. Furthermore, the osseointegration activity around the composite was higher than that around PEEK. In their study, the PEEK/cHAp composite was found to be more biocompatible and osseointegrable than PEEK. In another work, Faizal Manzoor et al. prepared PEEK-based filaments containing 10 wt. % of pure nanosized HA and PEEK/nano HA doped with Sr as well as Zn through hot-melt extrusion, which were subsequently 3D-printed via FDM [143]. Despite the reduction in crystallization temperature and increase in melting point with the addition of filler into pure PEEK, no noticeable changes in crystallinity were observed. Apart from the small drop in the tensile strength (~14%) and Young's modulus of approximately 5% in the PEEK/HA in comparison to the pure polymeric phase, the composites showed only slight differences in mechanical properties with the addition of the inorganic phases into the PEEK matrix. Moreover, the formation of apatite was observed on the surfaces of samples containing all the tested fillers, such as nano HA, SrHA and Zn HA. The in vitro bioactivity of 3D-printed samples was evaluated via a simulated body fluid immersion test for up to 28 days (Figure 5j) [143]. Zheng et al. reported the 3D printing of a PEEK/HA composite using a composite filament [144]. The composite filament was prepared through mechanical mixing followed by extrusion with filler loading of up to 30%. The HA phase was uniformly distributed on the surface of the PEEK matrix. A high amount of particle agglomeration was observed at this maximum filler loading. The strength and failure strain decreased with increasing HA content, whereas the modulus increased. The tensile modulus of the composite increased by around 68% when the HA content was increased to 30 wt. %. The tensile strength and elongation were highest for parts printed in the horizontal direction.

Recently, in 2020, Sikder et al. developed a melt blended amorphous magnesium phosphate (AMP) PEEK composite for dental AM manufacturing as well as orthopedic implants [145]. Osteogenic gene expression, cell viability, and proliferation were studied using mouse pre-osteoblasts (MC3T3-E1). Pure PEEK was used for in vivo analyses. The results show a homogeneous mixing of AMP particles within the matrix based on PEEK, with no degradation of the phase. AMP-PEEK composites exhibit low shear viscosities, which are suitable for 3D printing. The bioactivity was found to be improved with an increase in pre-osteoblast adhesion and proliferation through the incorporation of AMP in the PEEK matrix. Important gene expression markers like type I collagen (Col1), osteocalcin (OCN) and osteopontin (OPN) were increased by the presence of magnesium ions. In addition, AMP-filled PEEK composites exhibited enhanced osseointegration with a significant increase in new bone formation surrounding the composite implants. Even though PEEK filled with HA are the most studied and utilized materials for the development of scaffolds, several other materials were also studied to assess their ability to support tissue engineering. Even though FDM is a rapidly growing 3D printing technology, the mechanical properties and biocompatibility of FDM-printed PEEK and its composites need further investigation. Han et al. examined the printing of carbon fiber-reinforced PEEK (CFR-PEEK) composite using FDM and evaluated the resulting sample's mechanical properties [146]. In general, the printed CFR-PEEK composites were found to have higher mechanical tensile and bending strengths than the pure PEEK, without compromising much in terms of compressive strength. The cytotoxicity studies indicated that the printing process generated non-toxic effects even after 24 h of incubation. The carbon fiber reinforce-

ment could improve mechanical properties, while having little influence on cytotoxicity and cell adhesion. Fahad et al. fabricated PEEK composites filled with both CNTs and graphene nanoplatelets (GNPs) [147]. It was reported that the 3D-printed PEEK nanocomposites maintained the desired degree of crystallinity with enhanced mechanical properties. An increase in the bioactivity and appetite growth in SBF was noticed for the reinforcements with CNT and GNP, which could be described by the ion's electrostatic interaction in SBF with SO_3H, a functional group generated by sulfonation.

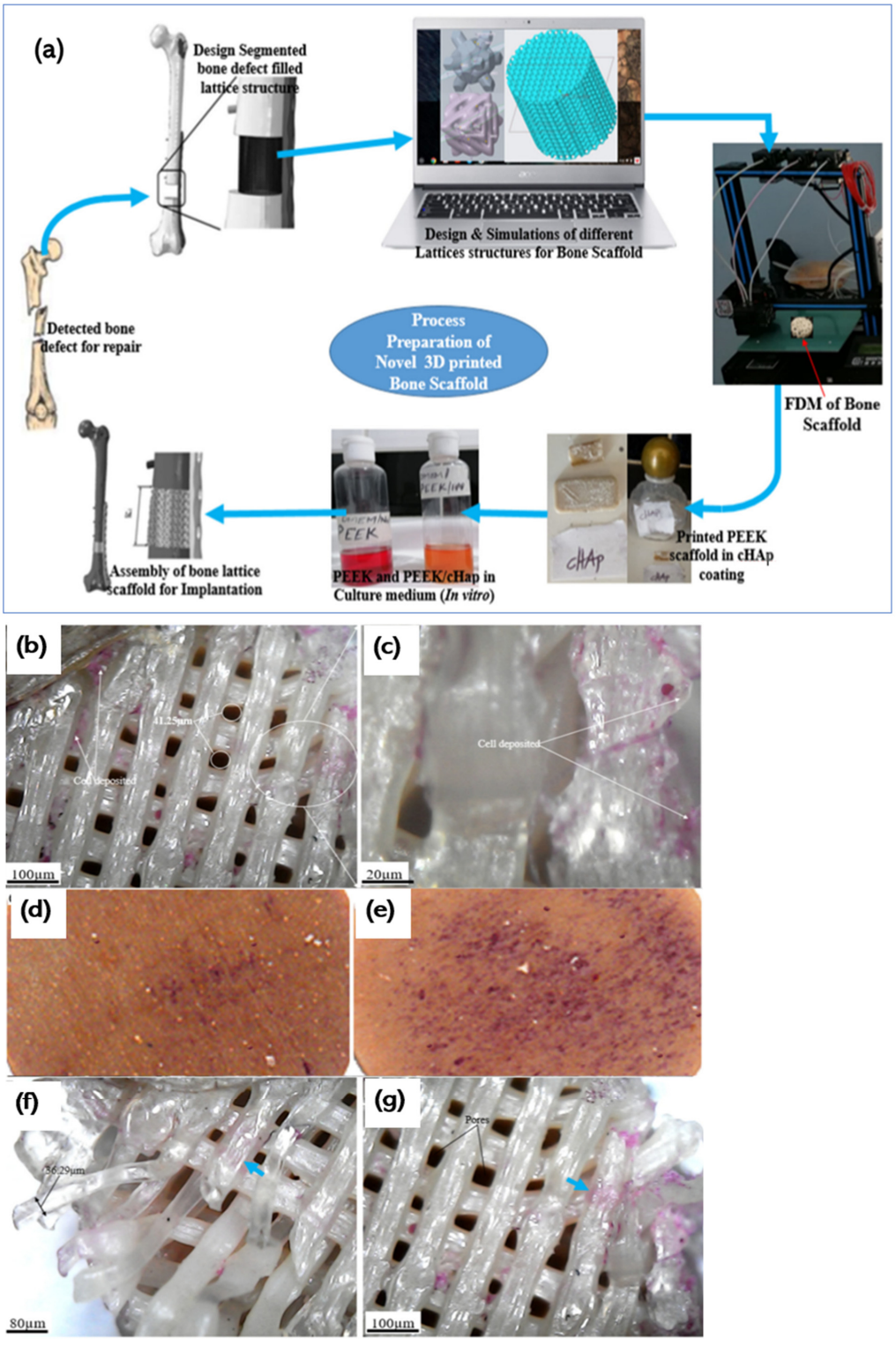

Figure 5. *Cont.*

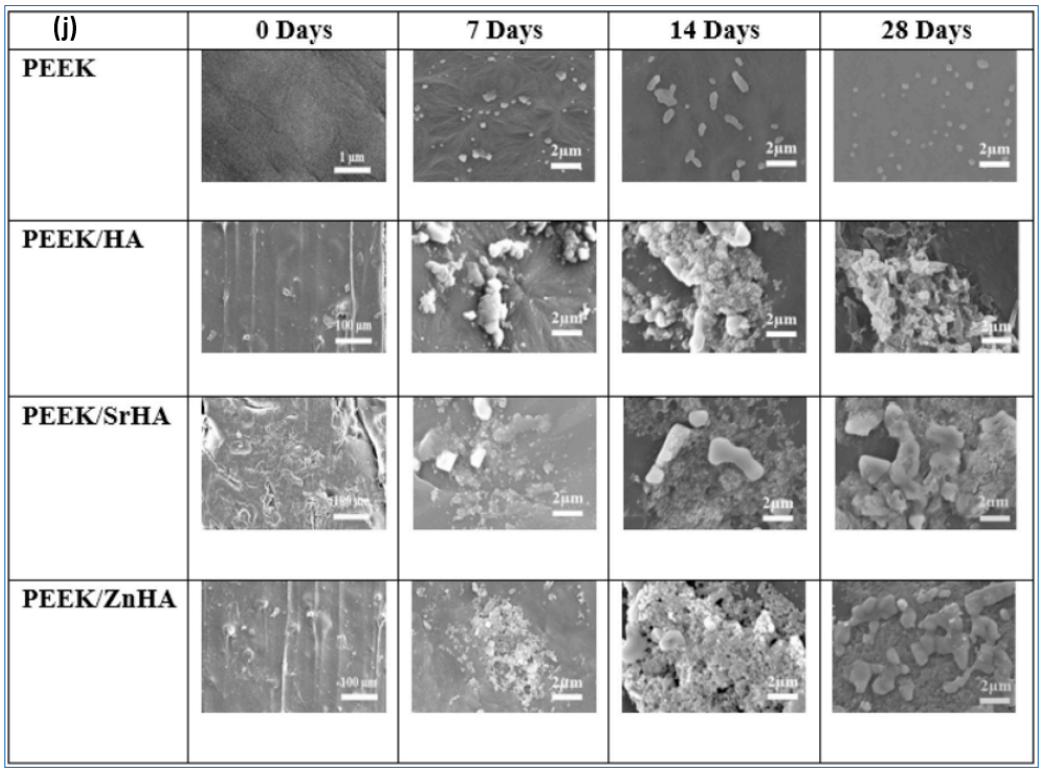

Figure 5. (**a**) Schematic of PEEK-based bone implant printed using FDM. (**b**–**g**) Cell attachment to the surface of the PEEK and PEEK and cHAp scaffold [137]. Copyright © 2020 with permission from Elsevier. (**j**) SEM micrographs of apatite layer development on the PEEK and PEEK composite surface after keeping them in a simulated body fluid for different days [143]. Copyright © 2021 with permission from Elsevier.

To ensure mechanical suitability for medical implants, Petersmann et al. studied various 3D-printable polymers, such as PLA, PEEK, polypropylene (PP), poly(methyl methacrylate) (PMMA), poly(vinylidene fluoride) (PVDF) and glycol-modified poly(ethylene terephthalate) (PETG), and in the temperature range desired for specific applications [148]. The high strength of PMMA and PEEK makes them suitable for load-bearing components; for example, cranial implants [149–151]. However, PP and PVDF show high flexibility, which could make them suitable for the sutural material application [152]. Pierantozzi et al. fabricated scaffolds based on PCL, PCL-HA and PCL-Sr HA using the FDM technique (Figure 6) [153]. Based on micro-CT analysis (Figure 6a), it became evident that the different designs produced showed high fidelity to the CAD model in terms of the porosity values (which were in the range of cancellous bone). Micro-CT and scanning electron microscopy (SEM) together confirm the uniform dispersion of ceramic particles within the PCL matrix, both on the surface and in the interior. These scaffolds also show good biocompatibility and support for cell growth, attachment, and proliferation. Among the studied composites, the SrHA-based scaffold showed high mineralization when compared to the PCL-HA and PCL-based scaffolds. In terms of mechanical properties, mineralization plays a key role. The use of mineralized micro- or nanomaterials in composites will enhance the mechanical properties of biomaterials and mimic the functions of natural bone tissue. Therefore, the authors of this study suggested that SrHA-based composites would be an attractive candidate for the development of bone scaffolds in tissue engineering.

Several other biocompatible polymers have been examined to make composites using different fillers, such as HA carbonated HA and nano HA. These composites show good wettability from biological fluids. It is pointed out by several authors that the degree of crystallinity and glass transition temperature were almost independent of the filler content [154–156]. Modal et al. reported the development of nanocomposite-based biomaterials containing acrylated epoxidized soyabean oil, PEGDA, and nano HA through the masked stereolithography (mSLA) technique for tissue engineering applications. The developed composites showed chemical stability, mechanical stability, good viability, and the proliferation of osteoblasts that differentiated from the mouse pre-osteoblast, MC3T3-E1 [157]. PCL in combination with PLGA and tricalcium phosphate in a particular ratio (i.e., 4:4:2) showed superior bone restoration capability [158]. However, PEEK-based composites have a combination of advantages over alternatives, which make them an excellent choice as a bone scaffold material, including their excellent biocompatibility, low density (1.32 g/cm^3), chemical resistance, and mechanical properties that better match human bone.

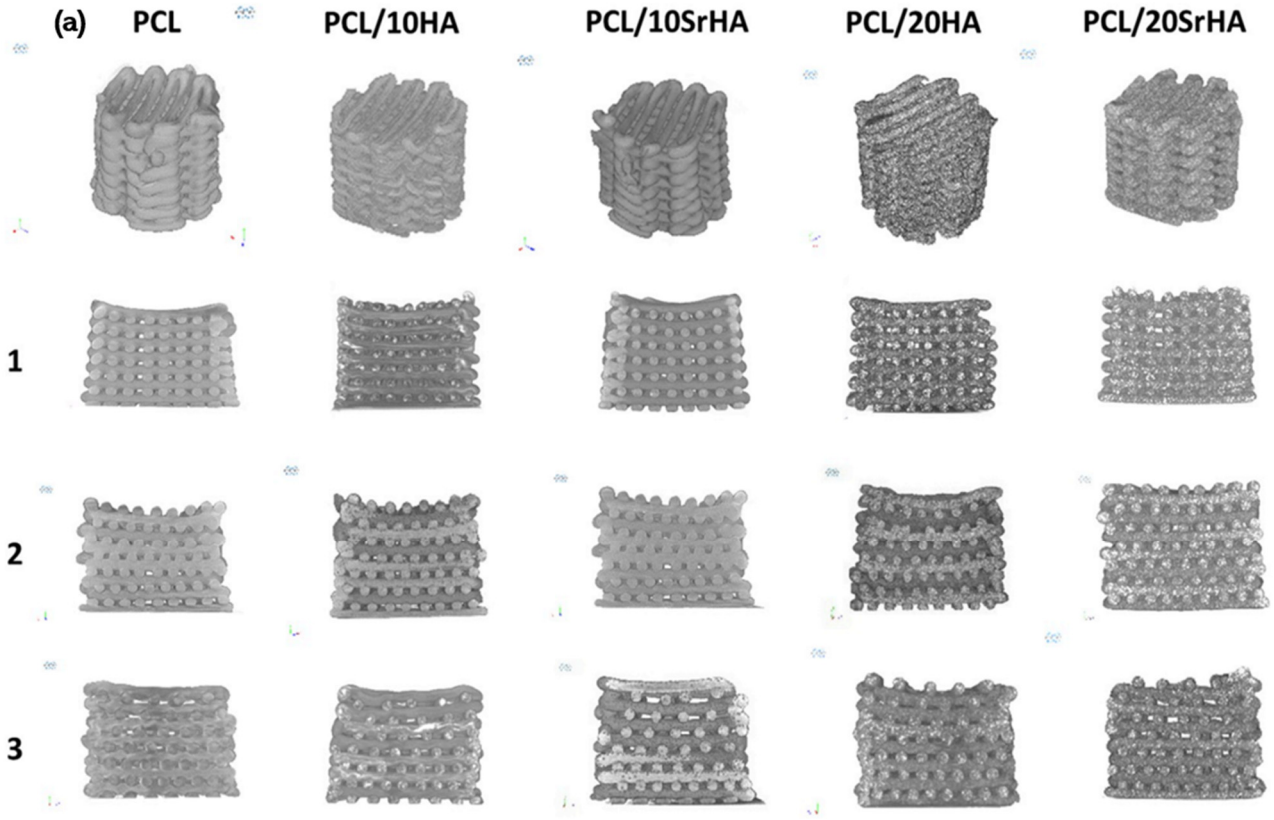

Figure 6. *Cont.*

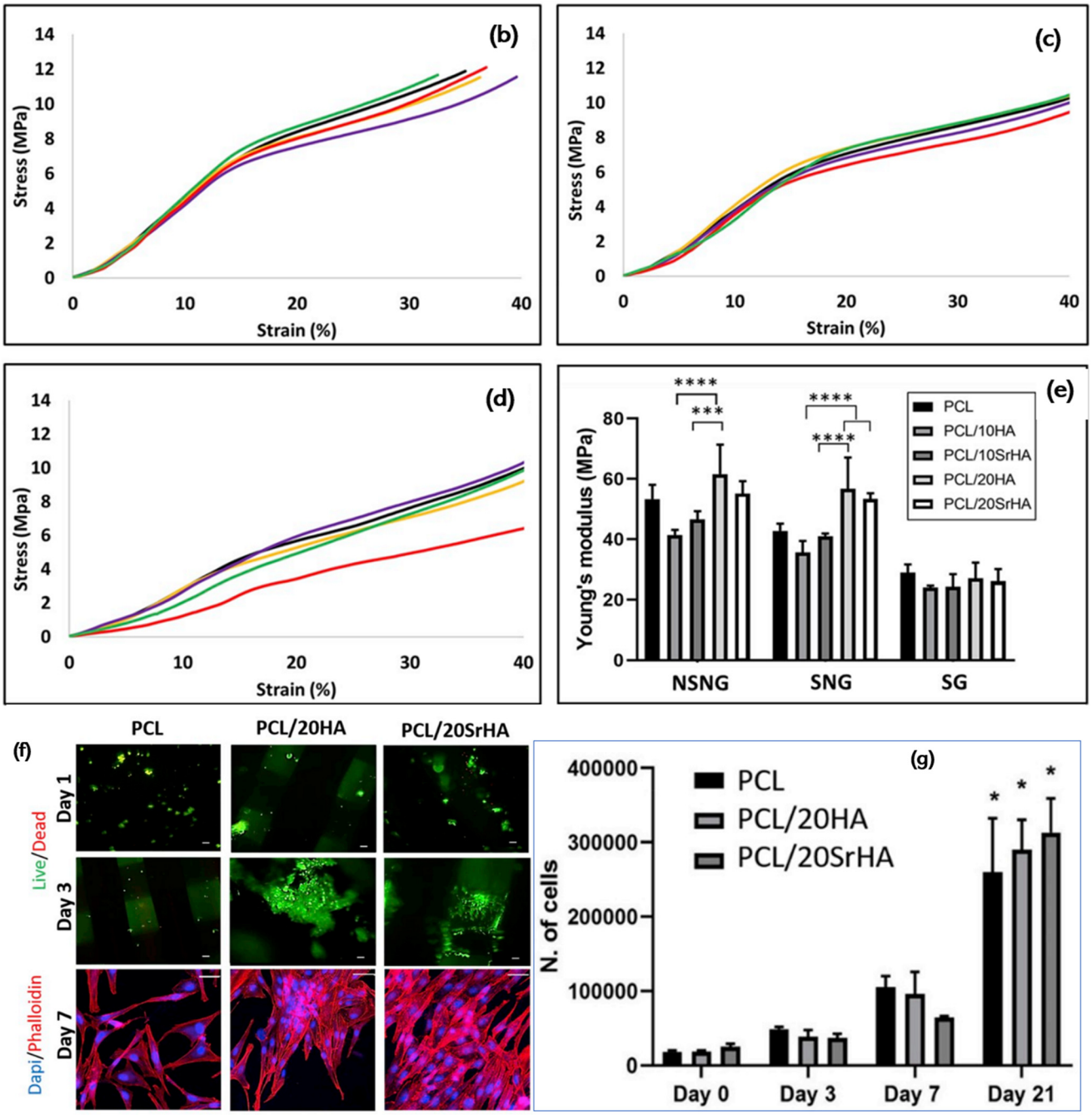

Figure 6. (**a**) Micro-CT pictures of 3D-printed scaffolds. (**b**–**d**) Compressive stress–strain curves of 3D-printed PCL scaffolds (black line), PCL and 10HA (purple line), PCL and 10SrHA (yellow line), PCL and 20HA (green line), and PCL and 20SrHA (red line) and (**e**) Young's modulus values (statistics: $p < 0.0001$ (****), p $\frac{1}{4}$ 0.0005 (***)). (**f**) Evaluation of cytocompatibility of 3D-printed scaffolds based on PCL, PCL/20HA and PCL and 20SrHA. (**g**) Cell number count and standard calibration curve (statistics: $p < 0.0001$ (*)) [153]. Copyright © 2021 with permission from Elsevier.

3. Conclusions

This article reviewed the recent developments in the PEEK composites-based scaffolds developed using 3D printing methods and summarized the mechanical, biological, and biophysical properties of scaffolds for tissue engineering using pure PEEK as well as PEEK composites. It is shown how PEEK osteointegration is accelerated by surface coatings that incorporate bioactive HA with different particle morphologies. Recent studies show that PEEK-based composites are the ideal choice to scaffold 3D printing due to their

biocompatibility, low density, and good mechanical characterization, which match well with natural bone. The cytotoxicity of materials is an important consideration when selecting materials for tissue engineering applications. The cytotoxicity of PEEK can be tailored using appropriate filler materials, which is an advantage. The material has potential for tissue engineering applications, but there are issues like weak bonding between PEEK implants and surrounding tissues. The problem is expected to be solved by using innovative PEEK-based composites and porous structures. Thus, more research is needed to resolve this issue and to allow this material to be applied more in tissue engineering. The use of 3D printing technology in scaffold fabrication when compared to traditional techniques provides advantages such as the ability to create versatile and customized scaffolds with highly complex architectures, and to mimic the extracellular matrix. However, 3D-printed implants based on PEEK have yet to be commercialized. Prior to the clinical translation of 3D-printed customized PEEK implants, some obstacles need to be overcome in terms of regulation and technical standards. Clinical translation is currently hindered by a lack of technical data.

Author Contributions: Conceptualization, R.S.; writing—original draft preparation, R.S., A.B., S.V. and S.S.P.; writing—review and editing, D.B. and K.M. All authors have read and agreed to the published version of the manuscript.

Funding: Science Foundation Ireland: 16/1571 RC/3872, 19/US-C2C/3579; Erasmus + KA107 ICM: IRLDUBLIN04.

Data Availability Statement: Data are contained within the article.

Conflicts of Interest: The authors declare no conflict of interest.

References

1. Ngo, T.D.; Kashani, A.; Imbalzano, G.; Nguyen, K.T.Q.; Hui, D. Additive manufacturing (3D printing): A review of materials, methods, applications and challenges. *Compos. Part B Eng.* **2018**, *143*, 172–196. [CrossRef]
2. Gibson, I.; Rosen, D.W.; Stucker, B. *Additive Manufacturing Technologies*; Springer: New York, NY, USA, 2015.
3. Rafiee, M.; Farahani, R.D.; Therriault, D. Multi-Material 3D and 4D Printing: A Survey. *Adv. Sci.* **2020**, *7*, 1902307. [CrossRef] [PubMed]
4. Goh, G.L.; Zhang, H.; Chong, T.H.; Yeong, W.Y. 3D Printing of Multilayered and Multimaterial Electronics: A Review. *Adv. Electron. Mater.* **2021**, *7*, 2100445. [CrossRef]
5. Anketa, J.; Ikshita, C.; Ishika, W.; Ankush, R.; Mir, I.U.-H. 3D printing—A review of processes, materials and applications in industry 4.0. *Sustain. Oper. Comput.* **2022**, *3*, 33–42.
6. Qi, X.B.; Chen, G.F.; Li, Y.; Cheng, X.; Li, C.P. Applying Neural-Network-Based Machine Learning to Additive Manufacturing: Current Applications, Challenges, and Future Perspectives. *Engineering* **2019**, *5*, 721–729. [CrossRef]
7. Wang, C.; Tan, X.P.; Tor, S.B.; Lim, C.S. Machine learning in additive manufacturing: State-of-the-art and perspectives. *Addit. Manuf.* **2020**, *36*, 101538. [CrossRef]
8. Qin, J.; Hu, F.; Liu, Y.; Witherell, P.; Wang, C.C.L.; Rosen, D.W.; Simpson, T.W.; Lu, Y.; Tang, Q. Research and application of machine learning for additive manufacturing. *Addit. Manuf.* **2022**, *52*, 102691. [CrossRef]
9. Aboulkhair, N.T.; Everitt, N.M.; Ashcroft, I.; Tuck, C. Reducing porosity in AlSi10Mg parts processed by selective laser melting. *Addit. Manuf.* **2014**, *1*, 77–86. [CrossRef]
10. Liu, T.; Guessasma, S.; Zhu, J.; Zhang, W.; Nouri, H.; Belhabib, S. Microstructural defects induced by stereolithography and related compressive behaviour of polymers. *J. Mater. Process. Technol.* **2018**, *251*, 37–46. [CrossRef]
11. Sing, S.L.; Wiria, F.E.; Yeong, W.Y. Selective laser melting of titanium alloy with 50 wt% tantalum: Effect of laser process parameters on part quality. *Int. J. Refract. Metal Hard Mater.* **2018**, *77*, 120–127. [CrossRef]
12. Froes, F.; Boger, R. *Additive Manufacture for Aerospace Industry*; Elsevier: Alpharetta, GA, USA, 2019; pp. 1–6.
13. Charles, A.; Hofer, A.; Elkaseer, A.; Scholz, S.G. Additive Manufacturing in the Automotive Industry and the Potential for Driving the Green and Electric Transition. *Smart Innov. Syst. Technol.* **2022**, *262*, 339–346.
14. Li, C.; Pisignano, D.; Zhao, Y.; Xue, J. Advances in Medical Applications of Additive Manufacturing. *Engineering* **2020**, *6*, 1222–1231. [CrossRef]
15. Sreenilayam, S.P.; Ul Ahad, I.; Nicolosi, V.; Garzon, V.A.; Brabazon, D. Advanced materials of printed wearables for physiological parameter monitoring. *Mater. Today* **2020**, *32*, 147. [CrossRef]
16. Sreenilayam, S.P.; Ul Ahad, I.; Nicolosi, V.; Brabazon, D. MXene materials based printed flexible devices for healthcare, biomedical and energy storage applications. *Mater. Today* **2021**, *43*, 99–131. [CrossRef]

17. Tom, T.; Sreenilayam, S.P.; Brabazon, D.; Jose, J.P.; Joseph, B.; Madanan, K.; Thomas, S. Additive manufacturing in the biomedical field-recent research developments. *Results Eng.* **2022**, *16*, 100661. [CrossRef]
18. Obeidi, M.A. Metal additive manufacturing by laser-powder bed fusion: Guidelines for process optimisation. *Results Eng.* **2022**, *15*, 100473. [CrossRef]
19. Langer, R.; Tirrell, D.A. Designing materials for biology and medicine. *Nature* **2004**, *428*, 487–492. [CrossRef]
20. Chan, B.P.; Leong, K.W. Scaffolding in tissue engineering: General approaches and tissue-specific considerations. *Eur. Spine J.* **2008**, *17*, 467–479. [CrossRef]
21. Nikolova, M.P.; Chavali, M.S. Recent advances in biomaterials for 3D scaffolds: A review. *Bioact. Mater.* **2019**, *4*, 271–292. [CrossRef]
22. Chen, M.; Le, D.Q.; Baatrup, A.; Nygaard, J.V.; Hein, S.; Bjerre, L.; Kassem, M.; Zou, X.; Bunger, C. Self-assembled composite matrix in a hierarchical 3-D scaffold for bone tissue engineering. *Acta Biomater.* **2011**, *7*, 2244. [CrossRef]
23. Peter, S.J.; Miller, M.J.; Yasko, A.W.; Yaszemski, M.J.; Mikos, A.G. Polymer concepts in tissue engineering. *J. Biomed. Mater. Res.* **1998**, *43*, 422. [CrossRef]
24. Bose, S.; Vahabzadeh, S.; Bandyopadhyay, A. Bone tissue engineering using 3D printing. *Mater. Today* **2013**, *16*, 496. [CrossRef]
25. Liu, W.Y.; Li, Y.; Liu, J.Y.; Niu, X.F.; Wang, Y.; Li, D.Y. Application and Performance of 3D Printing in Nanobiomaterials. *J. Nanomater.* **2013**, *2013*, 681050. [CrossRef]
26. Taboas, J.M.; Maddox, R.D.; Krebsbach, P.H.; Hollister, S. Indirect solid free form fabrication of local and global porous, biomimetic and composite 3D polymer-ceramic scaffolds. *J. Biomater.* **2003**, *24*, 181. [CrossRef]
27. Mikos, A.; Temenoff, J. Formation of highly porous biodegradable scaffolds for tissue engineering. *Electron. J. Biotechnol.* **2000**, *3*, 23. [CrossRef]
28. Whang, K.; Thomas, C.; Healy, K.; Number, G. A novel method to fabricate bioabsorbable scaffolds. *Polymer* **1995**, *36*, 837. [CrossRef]
29. O'Brien, F.J.; Harley, B.A.; Yannas, I.V.; Gibson, L. Influence of freezing rate on pore structure in freeze-dried collagen-GAG scaffolds. *Biomaterials* **2004**, *25*, 1077. [CrossRef] [PubMed]
30. Ma, P.X.; Langer, R. Fabrication of biodegradable polymer foams for cell transplantation and tissue engineering. *Methods Mol. Med.* **1999**, *18*, 47.
31. Ma, P.X. Scaffolds for tissue fabrication. *Mater. Today* **2004**, *7*, 30. [CrossRef]
32. Nam, Y.S.; Yoon, J.J.; Park, T.G. A novel fabrication method of macroporous biodegradable polymer scaffolds using gas foaming salt as a porogen additive. *J. Biomed. Mater. Res.* **2000**, *53*, 1. [CrossRef]
33. Keskar, V.; Marion, N.W.; Mao, J.J.; Gemeinhart, R.A. In vitro evaluation of macroporous hydrogels to facilitate stem cell infiltration, growth, and mineralization. *Tissue Eng. Part A* **2009**, *15*, 1695. [CrossRef] [PubMed]
34. Salerno, A.; Di Maio, E.; Iannace, S.; Netti, P. Tailoring the pore structure of PCL scaffolds for tissue engineering prepared via gas foaming of multi-phase blends. *J. Porous Mater.* **2012**, *19*, 181. [CrossRef]
35. Karageorgiou, V.; Kaplan, D. Porosity of 3D biomaterial scaffolds and osteogenesis. *Biomaterials* **2005**, *26*, 5474. [CrossRef] [PubMed]
36. Hollister, S. Porous scaffold design for tissue engineering. *Nat. Mater.* **2005**, *4*, 518. [CrossRef]
37. Cubo-Mateo, N.; Rodríguez-Lorenzo, L.M. Design of Thermoplastic 3D-Printed Scaffolds for Bone Tissue Engineering: Influence of Parameters of "Hidden" Importance in the Physical Properties of Scaffolds. *Polymers* **2020**, *12*, 1546. [CrossRef]
38. Mitra, A.-E.; Trevor, C.B.; Ali, B. RAFT-Mediated 3D Printing of "Living" Materials with Tailored Hierarchical Porosity. *ACS Appl. Polym. Mater.* **2022**, *4*, 4940.
39. Li, Z.; Du, T.; Gao, C.; Tang, L.; Chen, K.; Liu, J.; Yang, J.; Zhao, X.; Niu, X.; Ruan, C. In-situmineralized homogeneous collagen-based scaffolds for potential guided bone regeneration. *Biofabrication* **2022**, *14*, 045016. [CrossRef]
40. Vasconcellos, L.M.R.D.; Oliveira, M.V.D.; Graça, M.L.D.A.; Vasconcellos, L.G.O.D.; Carvalho, Y.R.; Cairo, C.A.A. Porous Titanium Scaffolds Produced by Powder Metallurgy for Biomedical Applications. *Mater. Res.* **2008**, *11*, 275. [CrossRef]
41. Chou, D.T.; Wells, D.; Hong, D.; Lee, B.; Kuhn, H.; Kumta, P.N. Novel processing of iron–manganese alloy-based biomaterials by inkjet 3-D printing. *Acta Biomater.* **2013**, *9*, 8593. [CrossRef]
42. Wataha, J.C.; Hobbs, D.T.; Wong, D.J.; Dogan, S.; Zhang, H.; Chung, K.H. Elvington, Titanates deliver metal ions to human monocytes. *J. Mater. Sci. Mater. Med.* **2010**, *21*, 1289. [CrossRef]
43. Davis, R.R.; Hobbs, D.T.; Khashaba, R.; Sehkar, P.; Seta, F.N.; Messer, R.L.; Lewis, J.B.; Wataha, J.C. Titanate particles as agents to deliver gold compounds to fibroblasts and monocytes. *J. Biomed. Mater. Res. Part A* **2010**, *93*, 864.
44. Jayakumar, R.; Ramachandran, R.; Divyarani, V.V.; Chennazhi, K.P.; Tamura, H.; Nair, S.V. Fabrication of chitin-chitosan/nano TiO2-composite scaffolds for tissue engineering applications. *Int. J. Biol. Macromol.* **2011**, *48*, 336. [CrossRef] [PubMed]
45. Balla, V.K.; Bodhak, S.; Bose, S.; Bandyopadhyay, A. Porous tantalum structures for bone implants: Fabrication, mechanical and in vitro biological properties. *Acta Biomater.* **2010**, *6*, 3349. [CrossRef] [PubMed]
46. Dabrowski, B.; Swieszkowski, W.; Godlinski, D.; Kurzydlowski, K.J. Highly porous titanium scaffolds for orthopaedic applications. *J. Biomed. Mater. Res. Part B Appl. Biomater.* **2010**, *95*, 53. [CrossRef] [PubMed]
47. Zhuang, H.; Han, Y.; Feng, A. Preparation, mechanical properties and *in vitro* biodegradation of porous magnesium scaffolds. *Mater. Sci. Eng. C* **2008**, *28*, 1462. [CrossRef]

48. Vorndran, E.; Wunder, K.; Moseke, C.; Biermann, I.; Muller, F.A.; Zorn, K.; Gbureck, U. Hydraulic setting $Mg_3(PO_4)_2$ powders for 3D printing technology. *Adv. Appl. Ceram.* **2011**, *110*, 476. [CrossRef]
49. Seitz, H.; Rieder, W.; Irsen, S.; Leukers, B.; Tille, C. Three-dimensional printing of porous ceramic scaffolds for bone tissue engineering. *J. Biomed. Mater. Res. Part B Appl. Biomater.* **2005**, *74*, 782. [CrossRef]
50. Wu, C.; Fan, W.; Zhou, Y.; Luo, Y.; Gelinsky, M.; Chang, J.; Xiao, Y. 3D-printing of highly uniform $CaSiO_3$ ceramic scaffolds: Preparation, characterization, and *in vivo* osteogenesis. *J. Mater. Chem.* **2012**, *22*, 12288. [CrossRef]
51. Roy, D.M.; Kurtossy, L.S. Hydroxyapatite formed from Coral Skeletal Carbonate by Hydrothermal Exchange. *Nature* **1974**, *247*, 220. [CrossRef]
52. Leukers, B.; Gulkan, H.; Irsen, S.H.; Milz, S.; Tille, C.; Schieker, M.; Seitz, H. Hydroxyapatite scaffolds for bone tissue engineering made by 3D printing. *J. Mater. Sci. Mater. Med.* **2005**, *16*, 1121. [CrossRef]
53. Warnke, P.H.; Seitz, H.; Warnke, F.; Becker, S.T.; Sivananthan, S.; Sherry, E.; Liu, Q.; Wiltfang, J.; Douglas, T. Ceramic scaffolds produced by computer-assisted 3D printing and sintering: Characterization and biocompatibility investigations. *J. Biomed. Mater. Res. Part B Appl. Biomater.* **2010**, *93*, 212. [CrossRef] [PubMed]
54. Detsch, R.; Schaefer, S.; Deisinger, U.; Ziegler, G.; Seitz, H.; Leukers, B. In Vitro-Osteoclastic Activity Studies on Surfaces of 3D Printed Calcium Phosphate Scaffolds. *J. Biomater. Appl.* **2011**, *26*, 359. [CrossRef] [PubMed]
55. Zhou, Z.; Buchanan, F.; Mitchell, C.; Dunne, N. Printability of calcium phosphate: Calcium sulphate powders for the application of tissue engineered bone scaffolds using the 3D printing technique. *Mater. Sci. Eng. C* **2014**, *38*, 1. [CrossRef] [PubMed]
56. Castilho, M.; Moseke, C.; Ewald, A.; Gbureck, U.; Groll, J.; Pires, I.; Teßmar, J.; Vorndran, E. Direct 3D powder printing of biphasic calcium phosphate scaffolds for substitution of complex bone defects. *Biofabrication* **2014**, *6*, 015006. [CrossRef] [PubMed]
57. Pugliese, R.; Beltrami, B.; Regondi, S.; Lunetta, C. Polymeric biomaterials for 3D printing in medicine: An overview. *Ann. 3D Print. Med.* **2021**, *2*, 100011. [CrossRef]
58. Billiet, T.; Gevaert, E.; De Schryver, T.; Cornelissen, M.; Dubruel, P. The 3D printing of gelatin methacrylamide cell-laden tissue-engineered constructs with high cell viability. *Biomaterials.* **2014**, *35*, 49. [CrossRef]
59. Hribar, K.C.; Soman, P.; Warner, J.; Chung, P.; Chen, S. Light-assisted direct-write of 3D functional biomaterials. *Lab Chip* **2014**, *14*, 268. [CrossRef]
60. Leong, K.F.; Cheah, C.M.; Chua, C.K. Solid freeform fabrication of three-dimensional scaffolds for engineering replacement tissues and organs. *Biomaterials* **2003**, *24*, 2363. [CrossRef]
61. Mountziaris, P.M.; Spicer, P.P.; Kasper, F.K.; Mikos, A.G. Harnessing and modulating inflammation in strategies for bone regeneration. *Tissue Eng. Part B Rev.* **2011**, *17*, 393. [CrossRef]
62. Rajan, V.; Murray, R. The duplicitous nature of inflammation in wound repair. *Wound Pract. Res.* **2008**, *16*, 122.
63. Sung, H.J.; Meredith, C.; Johnson, C.; Galis, Z.S. The effect of scaffold degradation rate on three-dimensional cell growth and angiogenesis. *Biomaterials* **2004**, *25*, 5735. [CrossRef] [PubMed]
64. Hong, J.M.; Kim, B.J.; Shim, J.H.; Kang, K.S.; Kim, K.J.; Rhie, J.W.; Cha, H.J.; Cho, D.W. Enhancement of bone regeneration through facile surface functionalization of solid freeform fabrication-based three-dimensional scaffolds using mussel adhesive proteins. *Acta Biomater.* **2012**, *8*, 2578. [CrossRef] [PubMed]
65. Inzana, J.A.; Olvera, D.; Fuller, S.M.; Kelly, J.P.; Graeve, O.A.; Schwarz, E.M.; Kates, S.L.; Awad, H.A. 3D printing of composite calcium phosphate and collagen scaffolds for bone regeneration. *Biomaterials* **2014**, *35*, 4026. [CrossRef] [PubMed]
66. Elangovan, S.; D'Mello, S.R.; Hong, L.; Ross, R.D.; Allamargot, C.; Dawson, D.V.; Stanford, C.M.; Johnson, G.K.; Sumner, D.R.; Salem, A.K. The enhancement of bone regeneration by gene activated matrix encoding for platelet derived growth factor. *Biomaterials* **2014**, *35*, 737. [CrossRef]
67. Bielajew, B.J.; Hu, J.C.; Athanasiou, K.A. Collagen: Quantification, biomechanics, and role of minor subtypes in cartilage. *Nat. Rev. Mater.* **2020**, *5*, 730. [CrossRef]
68. Lee, A.; Hudson, A.R.; Shiwarski, D.J.; Tashman, J.W.; Hinton, T.J.; Yerneni, S.; Bliley, J.M.; Campbell, B.G.; Feinberg, A.W. 3D bioprinting of collagen to rebuild components of the human heart. *Science* **2019**, *365*, 482–487. [CrossRef]
69. Li, X.H.; Zhu, X.; Liu, X.Y.; Xu, H.H.; Jiang, W.; Wang, J.J.; Chen, F.; Zhang, S.; Li, R.-X.; Chen, X.-Y.; et al. The corticospinal tract structure of collagen/silk fibroin scaffold implants using 3d printing promotes functional recovery after complete spinal cord transection in rats. *J. Mater. Sci. Mater. Med.* **2021**, *32*, 31. [CrossRef]
70. Lan, X.; Liang, Y.; Erkut, E.J.N.; Kunze, M.; Mulet-Sierra, A.; Gong, T.; Osswald, M.; Ansari, K.; Seikaly, H.; Boluk, Y.; et al. Bioprinting of human nasoseptal chondrocytes-laden collagen hydrogel for cartilage tissue engineering. *Faseb J.* **2021**, *35*, e21191. [CrossRef]
71. Serra, T.; Planell, J.A.; Navarro, M. High-resolution PLA-based composite scaffolds via 3-D printing technology. *Acta Biomater.* **2013**, *9*, 5521. [CrossRef]
72. Yadav, L.R.; Chandran, S.V.; Lavanya, K.; Selvamurugan, N. Chitosan-based 3D-printed scaffolds for bone tissue engineering. *Int. J. Biol. Macromol.* **2021**, *183*, 1925. [CrossRef]
73. Zhao, B.; Wang, H.; Qiao, N.; Wang, C.; Hu, M. Corrosion resistance characteristics of a Ti–6Al–4V alloy scaffold that is fabricated by electron beam melting and selective laser melting for implantation in vivo. *Mater. Sci. Eng. C* **2016**, *70*, 832. [CrossRef] [PubMed]

74. Yang, F.; Chen, C.; Zhou, Q.; Gong, Y.; Li, R.; Li, C.; Klämpfl, F.; Freund, S.; Wu, X.; Sun, Y.; et al. Laser beam melting 3D printing of Ti6Al4V based porous structured dental implants: Fabrication, biocompatibility analysis and photoelastic study. *Sci. Rep.* **2017**, *7*, 45360. [CrossRef] [PubMed]
75. Surmeneva, M.A.; Surmenev, R.A.; Chudinova, E.A.; Koptioug, A.; Tkachev, M.S.; Gorodzha, S.N.; Rännar, L.E. Fabrication of multiple-layered gradient cellular metal scaffold via electron beam melting for segmental bone reconstruction. *Mater. Des.* **2017**, *133*, 195. [CrossRef]
76. Fousová, M.; Kubásek, J.; Vojtěch, D.; Fort, J.; Čapek, J. 3D printed porous stainless steel for potential use in medicine. *IOP Conf. Ser. Mater. Sci. Eng.* **2017**, *179*, 012025. [CrossRef]
77. Igawa, K.; Mochizuki, M.; Sugimori, O.; Shimizu, K.; Yamazawa, K.; Kawaguchi, H.; Nakamura, K.; Takato, T.; Nishimura, R.; Suzuki, S.; et al. Tailor-made tricalcium phosphate bone implant directly fabricated by a three-dimensional ink-jet printer. *J. Artif. Organs.* **2006**, *9*, 234. [CrossRef]
78. Saijo, H.; Fujihara, Y.; Kanno, Y.; Hoshi, K.; Hikita, A.; Chung, U.; Takato, T. Clinical experience of full custom-made artificial bones for the maxillofacial region. *Regener. Ther.* **2016**, *5*, 72–78. [CrossRef]
79. Woldetsadik, A.D.; Sharma, S.K.; Khapli, S.; Jagannathan, R.; Magzoub, M. Hierarchically porous calcium carbonate scaffolds for bone tissue engineering. *ACS Biomater. Sci. Eng.* **2017**, *3*, 2457. [CrossRef]
80. Zhang, Y.; Shao, H.; Lin, T.; Peng, J.; Wang, A.; Zhang, Z.; Wang, L.; Liu, S.; Yu, X. Effect of Ca/P ratios on porous calcium phosphate salt bioceramic scaffolds for bone engineering by 3D gel-printing method. *Ceram. Int.* **2019**, *45*, 20493. [CrossRef]
81. Liu, Z.; Liang, H.; Shi, T.; Xie, D.; Chen, R.; Han, X.; Shen, L.; Wang, C.; Tian, Z. Additive manufacturing of hydroxyapatite bone scaffolds via digital light processing and in vitro compatibility. *Ceram. Int.* **2019**, *45*, 11079. [CrossRef]
82. Zhang, B.; Sun, H.; Wu, L.; Ma, L.; Xing, F.; Kong, Q.; Fan, Y.; Zhou, C.; Zhang, X. 3D printing of calcium phosphate bioceramic with tailored biodegradation rate for skull bone tissue reconstruction. *Bio-Des. Manuf.* **2019**, *2*, 161. [CrossRef]
83. Lee, U.L.L.; Lim, J.Y.Y.; Park, S.N.N.; Choi, B.H.H.; Kang, H.; Choi, W.C.C. A clinical trial to evaluate the efficacy and safety of 3D printed bioceramic implants for the reconstruction of zygomatic bone defects. *Materials* **2020**, *13*, 4515. [CrossRef] [PubMed]
84. Vijayavenkataraman, S.; Kuan, L.Y.; Lu, W.F. 3D-printed ceramic triply periodic minimal surface structures for design of functionally graded bone implants. *Mater. Des.* **2020**, *191*, 108602. [CrossRef]
85. Lindner, M.; Hoeges, S.; Meiners, W.; Wissenbach, K.; Smeets, R.; Telle, R.; Poprawe, R.; Fischer, H. Manufacturing of individual biodegradable bone substitute implants using selective laser melting technique. *J. Biomed. Mater. Res. A* **2011**, *97A*, 466. [CrossRef] [PubMed]
86. Tsai, C.H.; Hung, C.H.; Kuo, C.N.; Chen, C.Y.; Peng, Y.N.; Shie, M.Y. Improved bioactivity of 3D printed porous titanium alloy scaffold with chitosan/magnesium-calcium silicate composite for orthopaedic applications. *Materials* **2019**, *12*, 203. [CrossRef]
87. Nevado, P.; Lopera, A.; Bezzon, V.; Fulla, M.R.; Palacio, J.; Zaghete, M.A.; Biasotto, G.; Montoya, A.; Rivera, J.; Robledo, S.M.; et al. Preparation and in vitro evaluation of PLA/biphasic calcium phosphate filaments used for fused deposition modelling of scaffolds. *Mater. Sci. Eng. C* **2020**, *114*, 111013. [CrossRef]
88. Kobbe, P.; Laubach, M.; Hutmacher, D.W.; Alabdulrahman, H.; Sellei, R.M.; Hildebrand, F. Convergence of scaffold-guided bone regeneration and RIA bone grafting for the treatment of a critical-sized bone defect of the femoral shaft. *Eur. J. Med. Res.* **2020**, *25*, 70. [CrossRef]
89. Polley, C.; Distler, T.; Detsch, R.; Lund, H.; Springer, A.; Boccaccini, A.R.; Seitz, H. 3D printing of piezoelectric barium titanate-hydroxyapatite scaffolds with interconnected porosity for bone tissue engineering. *Materials* **2020**, *13*, 1773. [CrossRef]
90. Wang, W.; Zhang, B.; Li, M.; Li, J.; Zhang, C.; Han, Y.; Wang, L.; Wang, K.; Zhou, C.; Liu, L.; et al. 3D printing of PLA/n-HA composite scaffolds with customized mechanical properties and biological functions for bone tissue engineering. *Compos. B Eng.* **2021**, *224*, 109192. [CrossRef]
91. Mangano, C.; Giuliani, A.; De Tullio, I.; Raspanti, M.; Piattelli, A.; Iezzi, G. Case report: Histological and histomorphometrical results of a 3-D printed biphasic calcium phosphate ceramic 7 years after insertion in a human maxillary alveolar ridge. *Front. Bioeng. Biotechnol.* **2021**, *9*, 614325. [CrossRef]
92. Xu, T.; Binder, K.W.; Albanna, M.Z.; Dice, D.; Zhao, W.; Yoo, J.J.; Atala, A. Hybrid printing of mechanically and biologically improved constructs for cartilage tissue engineering applications. *Biofabrication* **2013**, *5*, 015001. [CrossRef]
93. Duan, B.; Kapetanovic, E.; Hockaday, L.A.; Butcher, J.T. Three-dimensional printed trileaflet valve conduits using biological hydrogels and human valve interstitial cells. *Acta Biomater.* **2014**, *10*, 1836. [CrossRef] [PubMed]
94. Kolesky, D.B.; Homan, K.A.; Skylar-Scott, M.A.; Lewis, J.A. Three-dimensional bioprinting of thick vascularized tissues. *Proc. Natl. Acad. Sci. USA* **2016**, *113*, 3179. [CrossRef] [PubMed]
95. Yeo, M.; Lee, J.S.; Chun, W.; Kim, G.H. An innovative collagen-based cell-printing method for obtaining human adipose stem cell-laden structures consisting of coresheath structures for tissue engineering. *Biomacromolecules* **2016**, *17*, 1365. [CrossRef] [PubMed]
96. Huang, S.; Yao, B.; Xie, J.; Fu, X. 3D bioprinted extracellular matrix mimics facilitate directed differentiation of epithelial progenitors for sweat gland regeneration. *Acta Biomater.* **2016**, *32*, 170. [CrossRef] [PubMed]
97. Chengzhu, L.; Yuchao, L.; Sie, C.T. Polyetheretherketone and Its Composites for Bone Replacement and Regeneration. *Polymers* **2020**, *12*, 2858.
98. Sun, C.; Kang, J.; Yang, C.; Zheng, J.; Su, Y.; Dong, E.; Liu, Y.; Yao, S.; Shi, C.; Pang, H.; et al. Additive manufactured polyether-ether-ketone implants for orthopaedic applications: A narrative review. *Biomater Transl.* **2022**, *3*, 116–133.

99. Ma, R.; Guo, D. Evaluating the bioactivity of a hydroxyapatite-incorporated polyetheretherketone biocomposite. *J. Orthop. Surg. Res.* **2019**, *14*, 1. [CrossRef]
100. Velisaris, C.N.; Seferis, J.C. Crystallization kinetics of polyetheretherketone (peek) matrices. *Polym. Eng. Sci.* **1986**, *26*, 1574. [CrossRef]
101. Lee, Y.; Porter, R.S.; Lin, J.S. On the double-melting behavior of poly (ether ether ketone). *Macromolecules* **1989**, *22*, 1756. [CrossRef]
102. Elise, F.M.; Ginu, U.U.; Amira, I.H. Bone Mechanical Properties in Healthy and Diseased States. *Annu. Rev. Biomed. Eng.* **2018**, *20*, 119–143.
103. Limmahakhun, S.; Oloyede, A.; Sitthiseripratip, K.; Xiao, Y.; Yan, C. Stiffness and strength tailoring of cobalt chromium graded cellular structures for stress-shielding reduction. *Mater. Des.* **2017**, *114*, 633–641. [CrossRef]
104. Liverani, E.; Rogati, G.; Pagani, S.; Brogini, S.; Fortunato, A.; Caravaggi, P. Mechanical interaction between additive-manufactured metal lattice structures and bone in compression: Implications for stress shielding of orthopaedic implants. *J. Mech. Behav. Biomed. Mater.* **2021**, *121*, 104608. [CrossRef] [PubMed]
105. Cebe, P.; Chung, S.Y.; Hong, S.D. Effect of thermal history on mechanical properties of polyetheretherketone below the glass transition temperature. *Appl. Polym. Sci.* **1987**, *33*, 487. [CrossRef]
106. Rajani, K.V.; Rajesh, S.; Murali, K.P.; Mohanan, P.; Ratheesh, R. Preparation and microwave characterization of PTFE/PEEK Blends. *Polym. Compos.* **2009**, *30*, 296. [CrossRef]
107. Burg, K.J.L.; Shalaby, S.W. PES and PEEK. In *Encyclopedia of Materials: Science and Technology*, 2nd ed.; Elsevier: Amsterdam, The Netherlands, 2001; pp. 6837–6839.
108. Jin, W.; Chu, P.K. Orthopedic Implants, Reference Module. In *Biomedical Sciences—Encyclopedia of Biomedical Engineering*; Elsevier: Amsterdam, The Netherlands, 2019; pp. 425–439.
109. Qin, L.; Yao, S.; Zhao, J.; Zhou, C.; Oates, T.W.; Weir, M.D.; Wu, J.; Xu, H.H.K. Review on Development and Dental Applications of Polyetheretherketone-Based Biomaterials and Restorations. *Materials* **2021**, *14*, 408. [CrossRef] [PubMed]
110. Schwitalla, A.D.; Zimmermann, T.; Spintig, T.; Kallage, I.; Müller, W.D. Fatigue limits of different PEEK materials for dental implants. *J. Mech. Behav. Biomed. Mater.* **2017**, *69*, 163. [CrossRef]
111. Mishra, S.; Chowdhary, R. PEEK materials as an alternative to titanium in dental implants: A systematic review. *Clin. Implant. Dent. Relat. Res.* **2019**, *21*, 208. [CrossRef]
112. Maldonado-Naranjo, A.L.; Healy, A.T.; Kalfas, I.H. Polyetheretherketone (PEEK) intervertebral cage as a cause of chronic systemic allergy: A case report. *Spine J.* **2015**, *5*, e1–e3. [CrossRef]
113. Basgul, C.; Yu, T.; MacDonald, D.; Siskey, R.; Marcolongo, M.; Kurtz, S. Structure-property relationships for 3D-printed PEEK intervertebral Lumbar cages produced using fused filament fabrication. *J. Mater. Res.* **2018**, *33*, 2040. [CrossRef]
114. Bakar, M.A.; Cheang, P.; Khor, K. Mechanical properties of injection molded hydroxyapatite-polyetheretherketone biocomposites. *Compos. Sci. Technol.* **2003**, *63*, 421. [CrossRef]
115. Bakar, M.A.; Cheng, M.; Tang, S.; Yu, S.; Liao, K.; Tan, C.; Khor, K.; Cheang, P. Tensile properties, tension–tension fatigue and biological response of polyetheretherketone–hydroxyapatite composites for load-bearing orthopedic implants. *Biomaterials* **2003**, *24*, 2245.
116. Converse, G.L.; Yue, W.; Roeder, R.K. Processing, and tensile properties of hydroxyapatite-whisker-reinforced polyetheretherketone. *Biomaterials* **2007**, *28*, 927. [CrossRef] [PubMed]
117. de Araújo Nobre, M.; Ferro, A.; Maló, P. Adult patient risk stratification using a risk score for periodontitis. *J. Clin. Med.* **2019**, *8*, 307. [CrossRef] [PubMed]
118. Garcia-Gonzalez, D.; Jayamohan, J.; Sotiropoulos, S.; Yoon, S.H.; Cook, J.; Siviour, C.; Arias, A.; Jerusalem, A. On the mechanical behaviour of PEEK and HA cranial implants under impact loading. *J. Mech. Behav. Biomed. Mater.* **2017**, *69*, 342. [CrossRef] [PubMed]
119. Wang, L.; Weng, L.; Song, S.; Sun, Q. Mechanical properties and microstructure of polyetheretherketone–hydroxyapatite nanocomposite materials. *Mater. Lett.* **2010**, *64*, 2201. [CrossRef]
120. Wang, L.; Weng, L.; Song, S.; Zhang, Z.; Tian, S.; Ma, R. Characterization of polyetheretherketone-hydroxyapatite nanocomposite materials. *Mater. Sci. Eng. A* **2011**, *528*, 3689. [CrossRef]
121. Yu, S.; Hariram, K.P.; Kumar, R.; Cheang, P.; Aik, K.K. In vitro apatite formation and its growth kinetics on hydroxyapatite/polyetheretherketone biocomposites. *Biomaterials* **2005**, *26*, 2343. [CrossRef]
122. Ma, R.; Tang, T. Current Strategies to Improve the Bioactivity of PEEK. *Int. J. Mol. Sci.* **2014**, *15*, 5426. [CrossRef]
123. Rinaldi, M.; Ghidini, T.; Cecchini, F.; Brandao, A.; Nanni, F. Additive layer manufacturing of poly (ether ether ketone) via FDM. *Compos. Part B Eng.* **2018**, *145*, 162. [CrossRef]
124. Jaafar, J.; Siregar, J.P.; Tezara, C.; Hazim, M.; Hamdan, M.; Rihayat, T. A review of important considerations in the compression molding process of short natural fiber composites. *Int. J. Adv. Manuf. Technol.* **2019**, *105*, 3437. [CrossRef]
125. Bastan, F.E. Fabrication and characterization of an electrostatically bonded PEEK-hydroxyapatite composites for biomedical applications. *J. Bio. Med. Mater. Res. B Appl. Bio Meter.* **2020**, *108*, 2513.
126. Conrad, T.L.; Roeder, R.K. Effects of porogen morphology on the architecture, permeability, and mechanical properties of hydroxyapatite whisker reinforced polyetheretherketone scaffolds. *J. Mech. Behav. Biomed. Mater.* **2020**, *106*, 103730. [CrossRef] [PubMed]

127. Deng, Y.; Liu, X.; Xu, A.; Wang, L.; Luo, Z.; Zheng, Y.; Deng, F.; Wei, J.; Tang, Z.; Wei, S. Effect of surface roughness on osteogenesis in vitro and osseointegration in vivo of carbon fiber-reinforced polyetheretherketone–nanohydroxyapatite composite. *Int. J. Nanomed.* **2015**, *10*, 1425.
128. Nisa, V.S.; Rajesh, S.; Murali, K.P.; Priyadersini, V.; Potty, S.N.; Ratheesh, R. Preparation, Characterization and Dielectric properties of temperature stable $SrTiO_3$/PEEK, composites for microwave substrate applications. *Compos. Sci. Technol.* **2008**, *68*, 106. [CrossRef]
129. Rego, B.T.; Neto, W.A.R.; de Paula, A.C.C.; Goes, A.M.; Bretas, R.E.S. Mechanical properties and stem cell adhesion of injection-molded poly (ether ether ketone) and hydroxyapatite nanocomposites. *J. Appl. Polym. Sci.* **2015**, *132*, 41748. [CrossRef]
130. Ventola, C.L. Medical applications for 3D printing: Current and projected uses. *Pharm. Ther.* **2014**, *39*, 704.
131. Saeed, K.; McIlhagger, A.; Harkin-Jones, E.; Kelly, J.; Archer, E. Predication of the in-plane mechanical properties of continuous carbon fibre reinforced 3D printed polymer composites using classical laminated-plate theory. *Compos. Struct.* **2021**, *259*, 113226. [CrossRef]
132. Berretta, S.; Davies, R.; Shyng, Y.; Wang, Y.; Ghita, O. Fused Deposition Modelling of high temperature polymers: Exploring CNT PEEK composites. *Polym. Test.* **2017**, *63*, 251. [CrossRef]
133. Wang, P.; Zou, B.; Ding, S.; Li, L.; Huang, C. Effects of FDM-3D printing parameters on mechanical properties and microstructure of CF/ PEEK and GF/PEEK. *Chinese J. Aeronotics* **2021**, *34*, 236. [CrossRef]
134. Schmidt, M.; Pohle, D.; Rechtenwald, T. Selective laser sintering of PEEK. *CIRP Ann.* **2007**, *56*, 205. [CrossRef]
135. Wang, P.; Zou, B.; Xiao, H.; Ding, S.; Huang, C. Effects of printing parameters of fused deposition modeling on mechanical properties, surface quality, and microstructure of PEEK. *J. Mater. Process. Technol.* **2019**, *271*, 62. [CrossRef]
136. Berretta, S.; Evans, K.; Ghita, O. Additive manufacture of PEEK cranial implants: Manufacturing considerations versus accuracy and mechanical performance. *Mater. Des.* **2018**, *139*, 141. [CrossRef]
137. Oladapo, B.I.; Ismail, S.O.; Bowoto, O.K.; Omigbodun, F.T.; Olawumi, M.A.; Muhammad, M.A. Lattice design and 3D-printing of PEEK with Ca10(OH)(PO4)3 and in-vitro bio-composite for bone implant. *Int. J. Biol. Macromol.* **2020**, *165*, 50. [CrossRef]
138. Rasheva, Z.; Zhang, G.; Burkhart, T.A. Correlation between the tribological and mechanical properties of short carbon fibers reinforced PEEK materials with different fiber orientations. *Tribol. Int.* **2010**, *43*, 1430. [CrossRef]
139. Evans, N.T.; Torstrick, F.B.; Lee, C.S.D.; Dupont, K.M.; Safranski, D.L.; Chang, W.A.; Macedo, A.E.; Lin, A.S.P.; Boothby, J.M.; Whittingslow, D.C.; et al. High-strength, surface-porous polyether-ether-ketone for load-bearing orthopedic implants. *Acta Biomater.* **2015**, *13*, 159. [CrossRef]
140. Hassanajili, S.; Karami-Pour, A.; Oryan, A.; Talaei-Khozani, T. Preparation and characterization of PLA/PCL/HA composite scaffolds using indirect 3D printing for bone tissue engineering. *Mater. Sci. Eng. C* **2019**, *104*, 109960. [CrossRef]
141. Chen, Q.; Liu, Y.; Yao, Q.Q.; Yu, S.S.; Zheng, K.; Pischetsrieder, M.; Boccaccini, A.R. Multi layered bioactive composite coating drug delivery capability by electrophoretic deposition combined with layer-by-layer deposition. *Adv. Biomater. Devices Med.* **2014**, *1*, 18.
142. Torres, Y.; Romero, C.; Chen, Q.; Pérez, G.; Rodríguez-Ortiz, J.A.; Pavón, J.J.; Álvarez, L.; Arévalo, C.; Boccaccini, A.R. Electrophoretic deposition of PEEK/45S5 bioactive glass coating on porous titanium substrate: Influence of processing conditions and porosity parameters. *Key Eng. Mater.* **2016**, *704*, 343. [CrossRef]
143. Manzoor, F.; Golbang, A.; Jindal, S.; Dixon, D.; McIlhagger, A.; Harkin-Jones, E.; Crawford, D.; Mancuso, E. 3D printed PEEK/HA composites for bone tissue engineering applications: Effect of material formulation on mechanical performance and bioactive potential. *J. Mech. Behav. Biomed. Mater.* **2021**, *121*, 104601. [CrossRef]
144. Zheng, J.; Kang, J.; Sun, C.; Yang, C.; Wang, L.; Li, D. Effects of printing path and material components on mechanical properties of 3D-printed polyether-ether-ketone/hydroxyapatite composites. *J. Mech. Behav. Biomed. Mater.* **2021**, *118*, 104475. [CrossRef]
145. Sikder, P.; Ferreira, J.A.; Ehsan, A.; Fakhrabadic Kantorski, K.Z.; Liberatore, M.W.; Bottino, M.C.; Bhaduri, S.B. Bioactive amorphous magnesium phosphate-polyetheretherketone composite filaments for 3D printing. *Dent. Mater.* **2020**, *36*, 865. [CrossRef] [PubMed]
146. Han, X.; Yang, D.; Yang, C.; Spintzyk, S.; Scheideler, L.; Li, P.; Li, D.; Geis-Gerstorfer, J.; Rupp, F. Carbon Fiber Reinforced PEEK Composites Based on 3D-Printing Technology for Orthopedic and Dental Applications. *J. Clin. Med.* **2019**, *8*, 240. [CrossRef] [PubMed]
147. Alam, F.; Varadarajan, K.M.; Koo, J.H.; Wardle, B.L.; Kumar, S. Additively Manufactured Polyetheretherketone (PEEK) with Carbon Nanostructure Reinforcement for Biomedical Structural Applications. *Adv. Eng. Mater.* **2020**, *22*, 2000483. [CrossRef]
148. Petersmann, S.; Spoerk, M.; De Steene, W.V.; Üçal, M.; Wiener, J.; Pinter, G.; Arbeiter, F. Mechanical properties of polymeric implant materials produced by extrusion-based additive manufacturing. *J. Mech. Behav. Biomed. Mater.* **2020**, *104*, 103611. [CrossRef]
149. Navarro, M.; Michiardi, A.; Castano, O.; Planell, J.A. Biomaterials in orthopaedics. *J. R. Soc. Interface* **2008**, *5*, 1137. [CrossRef]
150. Petersmann, S.; Spoerk, M.; Huber, P.; Lang, M.; Pinter, G.; Arbeiter, F. Impact optimization of 3D-printed poly(methyl metharylate) for cranial implants. *Macromol. Mater. Eng.* **2019**, *304*, 1900263. [CrossRef]
151. Panayotov, I.V.; Orti, V.; Cuisinier, F.; Yachouh, J. Polyetheretherketone (PEEK) for medical applications. *J. Mater. Sci. Mater. Med.* **2016**, *27*, 118. [CrossRef]
152. Ratner, B.D.; Hoffman, A.S.; Schoen, F.J.; Lemons, J.E. *Biomaterials Science: An Introduction to Materials in Medicin*, 2nd ed.; Elsevier: Amsterdam, The Netherlands, 2004.

153. Pierantozzi, D.; Scalzone, A.; Jindal, S.; Stıpniece, L.; Salma-Ancane, K.; Dalgarno, K.; Gentile, P.; Mancuso, E. 3D printed Sr-containing composite scaffolds: Effect of structural design and material formulation towards new strategies for bone tissue engineering. *Compos. Sci. Technol.* **2020**, *191*, 108069. [CrossRef]
154. Oladapoa, B.I.; Ismail, S.O.; Zahedi, M.; Khan, A.; Usman, H. 3D printing and morphological characterisation of polymeric composite scaffolds. *Eng. Struct.* **2020**, *216*, 110752. [CrossRef]
155. Petrovskaya, T.S.; Toropkov, N.E.; Mironov, E.G.; Azarmi, F. 3D printed biocompatible polylactidehydroxyapatite based material for bone implants. *Mater. Manuf. Process.* **2018**, *33*, 1899. [CrossRef]
156. Corcione, C.E.; Gervaso, F.; Scalera, F.; Montagna, F.; Sannino, A.; Maffezzol, A. The feasibility of printing polylactic acid–nanohydroxyapatite composites using a low-cost fused deposition modelling 3D printer. *J. Appl. Polym. Sci.* **2017**, *134*, 44656. [CrossRef]
157. Mondal, D.; Haghpanah, Z.; Huxman, C.J.; Tanter, S.; Sun, D.; Gorbet, M.; Willett, T.L. mSLA-based 3D printing of acrylated epoxidized soybean oil—nano-hydroxyapatite composites for bone repair. *Mater. Sci. Eng. C* **2021**, *130*, 112456. [CrossRef] [PubMed]
158. Hwang, K.S.; Choi, J.W.; Kim, J.H.; Chung, H.Y.; Jin, S.; Shim, J.H.; Yun, W.S.; Jeong, C.M.; Huh, J.B. Comparative Efficacies of Collagen-Based 3D Printed PCL/PLGA/β-TCP Composite Block Bone Grafts and Biphasic Calcium Phosphate Bone Substitute for Bone Regeneration. *Materials* **2017**, *10*, 421. [CrossRef] [PubMed]